Extended approximated Born-Oppenheimer equation. II. Application

Satrajit Adhikari,[1] Gert D. Billing,[1] Alexander Alijah,[2] Sheng H. Lin,[3] and Michael Baer[3,4,*]
[1]*Department of Chemistry, H.C. Ørsted Institute, University of Copenhagen, DK-2100 Ø, Copenhagen, Denmark*
[2]*Fakultät für Chemie, Universität Bielefeld, 33501 Bielefeld, Germany*
[3]*Institute of Atomic and Molecular Science, 10764 Taipei, Taiwan, Republic of China*
[4]*Department of Physics and Applied Mathematics, Soreq NRC, Yavne 81800, Israel*
(Received 10 December 1999; revised manuscript received 2 May 2000; published 15 August 2000)

In this work is applied the extended-approximated Born-Oppenheimer (BO) equation, as derived in the preceding article [Phys. Rev. A **62**, 032506, (2000)] to a tristate system. For this sake an appropriate scattering two-arrangement–two-coordinate model was devised. The calculations for each energy were done three times: once without doing any approximation, and two times by approximating the three coupled Schrödinger equations by two different, but gauge-related, single (extended) BO equation. State-to-state (reactive and nonreactive) transition probabilities were obtained, indicating that the new extended approximate BO equations yield relevant results for a tristate system.

PACS number(s): 31.30.−i, 31.15.−p, 03.65.−w

I. INTRODUCTION

In the preceding paper [1] (designated as I) a new approximated Born-Oppenheimer (BO) equation was derived. This equation is characterized by the fact that, in contrast to the ordinary BO equation, it also contains topological (or geometrical) effects due to nonadiabatic coupling terms. Following that derivation, we showed that for a two-state system this equation becomes the Baer-Englman equation, which was derived some time ago [2], and which was found to yield the correct state-to-state reactive transition probabilities for a two-dimensional–two-arrangement channel model [3–5]. In the present paper the newly formed extended BO equation will be applied to a tristate model, otherwise similar to the one that was used in the previous two-state calculation [3–5]. For this model we shall calculate the transition probabilities (both reactive and nonreactive) for energies below the upper excited states in several different ways: (1) A full tristate calculation which will be considered as the ''exact treatment.'' (2) Two single-state calculations, employing two different, extended approximate BO equations. (3) A ''relevant'' two-state calculation as will be explained later.

Recently two of the present authors carried out a detailed study of the topological effects related to a tristate model [6]. Among other things, efforts were made to reveal to what extent the topological effects of the decoupled two-state model are related to topological effects of the full (three-state) system. The topological effects for a two-state isolated system are presented in terms of an angle $\theta_{t12}(\varphi)$, the two-state adiabatic-diabatic-transformation (ADT) angle [7,8], which is obtained by integrating over $\tau_{12}(\varphi)$ (the nonadiabatic coupling term) that couples the ground and the first excited states [9–11]:

$$\theta_{t12}(\varphi)=\int_0^{\varphi}\tau_{12}(\varphi')d\varphi'. \tag{1}$$

Here φ stands for a nuclear angular coordinate defined in the range $[0, 2\pi]$. The topological effects for the full tristate model were presented in terms of an angle, $\theta_{12}(\varphi)$, which is derived by solving the Top-Baer system of three differential equations [11,12] which yield all three angles of the 3×3 ADT matrix. It was found that in some cases the two angles behave similarly and therefore will yield identical topological effects; however, there were other cases where they behave differently and the topological features were essentially ''opposite.'' The fact that Eq. (1) yields topological effects which are different from the actual ones is usually an indication that certain points of degeneracy, or a multidegeneracy at a give point, are not revealed by this expression. In this study, among other things, we shall show to what extent the failure to identify the correct topological features of a system will affect the final state-to-state transition probabilities.

In Sec. II we derive quantization conditions for the eigenvalues of the assumed nonadiabatic coupling matrix. In Sec. III we present the tristate model and the various Schrödinger equations that were solved to derive the transition probabilities. In Sec. IV we present and analyze the numerical results. In Sec. V we list the conclusions.

II. ''QUANTIZATION'' OF THE TRISTATE NONADIABATIC COUPLING MATRIX

In the present section we concentrate on an adiabatic tristate model. For this we first derive the quantization conditions to be fulfilled by the eigenvalues of nonadiabatic coupling matrix, and then the extended BO approximated equation.

The starting point is the 3×3 nonadiabatic matrix

$$\tau=\begin{pmatrix}0 & t_1 & t_2\\ -t_1 & 0 & t_3\\ -t_2 & -t_3 & 0\end{pmatrix}, \tag{2}$$

where t_j, $j=1,2,3$, are, at this stage, arbitrary functions of

*Guest professor at the Institute of Atomic and Molecular Science, Taipei, Taiwan.

 ©2000 The American Physical Society

the nuclear coordinates. The matrix G that diagonalizes τ at a given point in configuration space is of the form

$$G=\frac{1}{\bar{\omega}\lambda\sqrt{2}}\begin{pmatrix} it_2\bar{\omega}-t_3t_1 & -it_2\bar{\omega}-t_3t_1 & t_3\lambda\sqrt{2} \\ it_3\bar{\omega}+t_2t_1 & -it_3\bar{\omega}+t_2t_1 & -t_2\lambda\sqrt{2} \\ \lambda^2 & \lambda^2 & t_1\lambda\sqrt{2} \end{pmatrix} \quad (3)$$

where λ and $\bar{\omega}$ are defined as

$$\lambda=\sqrt{t_2^2+t_3^2}, \quad \bar{\omega}=\sqrt{t_1^2+t_2^2+t_3^2},$$

and the three eigenvalues are $(0,\pm i\bar{\omega})$. Assuming now that the τ matrix fulfills the conditions in Eqs. (5) and (6) given in I [these conditions ensure that the matrix G that diagonalizes $\tau(s)$ along a closed path is independent of s] we obtain, employing Eq. (26′) in I, the following topological D matrix [13] [the D matrix was introduced in I—see Eqs. (17), (26), and (26′)]:

$$D=\bar{\omega}^{-2}\begin{pmatrix} t_3^2+(t_1^2+t_2^2)c_1 & t_1\bar{\omega}s_1-2t_2t_3s_2 & -\bar{\omega}t_2s_1+2t_1t_3s_2 \\ t_1\bar{\omega}s_1-2t_2t_3s_2 & t_2^2+(t_1^2+t_3^2)c_1 & -t_3\bar{\omega}s_1+2t_1t_2s_2 \\ \bar{\omega}t_2s_1+2t_1t_3s_2 & t_3\bar{\omega}s_1+2t_1t_2s_2 & t_1^2+(t_2^2+t_3^2)c_1 \end{pmatrix}, \quad (4)$$

where c_1, s_1, and s_2 are defined as

$$s_1=\sin\left(\oint\bar{\omega}\cdot\mathbf{ds}\right), \quad c_1=\cos\left(\oint\bar{\omega}\cdot\mathbf{ds}\right),$$

$$s_2=\sin^2\left(\frac{1}{2}\left(\oint\bar{\omega}\cdot\mathbf{ds}\right)\right). \quad (5)$$

It is important to realize that Eqs. (5) and (6) in I guarantee that the ratios $t_j/\bar{\omega}$; $j=1,2,3$ are independent of s. Next we note that D becomes diagonal if and only if

$$\frac{1}{2\pi}\oint\bar{\omega}\cdot\mathbf{ds}=\frac{1}{2\pi}\oint\sqrt{t_1^2+t_2^2+t_3^2}\cdot\mathbf{ds}=n, \quad (6)$$

where n is an integer. Moreover, Eq. (6) guarantees that D becomes the unit matrix. Equation (6) is reminiscent of a quantization condition. Similar ''quantization'' laws exist if one of the t_j's becomes zero (if two out of the three t_j's become zero, then we are back at the two-state case, and n is allowed to be half an integer).

III. SCHRÖDINGER EQUATION

A. Adiabatic framework

The numerical treatment will be applied to a two-coordinate system, with q being a radial coordinate and φ a polar coordinate. We start the presentation by considering the 3×3 *nonadiabatic* (vector) matrix τ, which in a two-coordinate system has two components, namely, τ_q and τ_φ. In what follows we assume that $\tau_q\equiv0$, and τ_φ will be written as [see Eq. (5) in I]

$$\boldsymbol{\tau}_\varphi=t_\varphi\mathbf{g}=\frac{t_0}{q}\mathbf{g}. \quad (7)$$

Here q is radial coordinate t_0 is, at this stage, a nonspecified constant and $\mathbf{g}$ is a 3×3 constant matrix of the form

$$\mathbf{g}=\begin{pmatrix} 0 & 1 & 0 \\ -1 & 0 & \eta \\ 0 & -\eta & 0 \end{pmatrix}, \quad (8)$$

where η is a constant. From Eqs. (7) and (8) it is noted that the τ matrix first couples the ground adiabatic state to the first excited state, and then this first excited state to the second excited state. No direct coupling is assumed between the ground state and the second excited state.

Next we present a full adiabatic coupled system of Schrödinger equations for the above 3×3 nonadiabatic coupling matrix model [see Eq. (4) in I]:

$$\left(T+u_1+\frac{t_0^2}{2mq^2}-E\right)\psi_1+\frac{t_0}{mq}\frac{\partial}{\partial\varphi}\psi_2-\frac{\eta t_0^2}{2mq^2}\psi_3=0,$$

$$\left(T+u_2+\frac{t_0^2(1+\eta^2)}{2mq^2}-E\right)\psi_2-\frac{t_0}{mq}\frac{\partial}{\partial\varphi}\psi_1+\frac{\eta t_0}{mq}\frac{\partial}{\partial\varphi}\psi_3=0, \quad (9)$$

$$\left(T+u_3+\frac{\eta^2t_0^2}{2mq^2}-E\right)\psi_3-\frac{\eta t_0}{mq}\frac{\partial}{\partial\varphi}\psi_2-\frac{\eta t_0^2}{2mq^2}\psi_1=0,$$

where T is the nuclear kinetic energy operator:

$$T=-\frac{1}{2m}\left(\frac{\partial^2}{\partial q^2}+\frac{1}{q}\frac{\partial}{\partial q}+\frac{1}{q^2}\frac{\partial^2}{\partial\varphi^2}\right). \quad (10)$$

We shall now distinguish between three cases:

(a) The case that both t_0 and η are zero. In this case, Eqs. (9) become

$$(T+u_1-E)\psi=0, \quad (9a)$$

which is the ordinary approximate BO equation.

(b) The case that η is zero but t_0 differs from zero. In this case Eqs. (9) become

$$\left(T+u_1+\frac{t_0^2}{2mq^2}-E\right)\psi_1+\frac{t_0}{mq}\frac{\partial}{\partial\varphi}\psi_2=0,$$
$$\left(T+u_2+\frac{t_0^2}{2mq^2}-E\right)\psi_2-\frac{t_0}{mq}\frac{\partial}{\partial\varphi}\psi_1=0, \tag{9b}$$

which is a coupled system for the two lowest adiabatic states. In the case that $t_0=\frac{1}{2}$, these equations become the relevant equations for a conical intersection which were recently studied by Baer *et al.* [3] and Adhikari and Billing [5]. In what follows, we assume that $t_0=\frac{1}{2}$.

(c) The third case is the case of a coupled system of three adiabatic equations as presented in Eqs. (9), but where η (which is a constant) is chosen so that the quantization condition given in Eqs. (6), is fulfilled. Inserting the following values for t_j, namely, $t_1=1/(2q)$, $t_2=0$, and $t_3(=\eta t_1)=\eta/(2q)$ into Eqs. (6) yields, for an arbitrary (integer) n, the following η values

$$\eta=\sqrt{4n^2-1} \quad \text{for} \quad n=1\Rightarrow\eta=\sqrt{3}. \tag{11}$$

It is important to reiterate that once t_0 is chosen to be equal to $\frac{1}{2}$, Eqs. (9) are physically relevant if and only if η is given by Eq. (11). In the present case, we assume $n=1$.

Our next task is to present the relevant *extended* approximate BO equation. For this purpose we consider the set of *uncoupled* equations as presented in Eq. (11) in I for the case $N=3$. The functions $i\omega_j$ that appear in these equations are the eigenvalues of the g matrix, given in Eq. (8) (of the present paper). By solving the relevant eigenvalue problem we obtain

$$\omega_1=2, \quad \omega_2=-2, \quad \omega_3=0,$$

so that Eqs. (11) in I become

$$\left(T+u_1+\frac{t_0^2\omega_j^2}{2mq^2}-E\right)\psi_1+\frac{t_0\omega_j}{mq}\frac{\partial}{\partial\varphi}\psi_2=0. \tag{12}$$

For $t_0=\frac{1}{2}$ and for various ω_j values, this set of uncoupled equations is a set of three gauge invariant equations, and therefore it is enough to solve only one of them. In the present study we solved them twice, once for $\omega_j=0$ and once for $\omega_j=2$. It is noted that for $\omega_j=0$, Eq. (12) becomes Eq. (9a), namely, the ordinary approximate BO equation. We also solved it for $\omega_j=2$, just to show that, indeed, we obtain similar results to those for $\omega_j=0$.

As mentioned earlier, we shall compare the present three-state results, with results due to two-state calculations. The relevant system of equations for this case is the one given in Eq. (9b), where again $t_0=\frac{1}{2}$. In addition, for completeness, we will present results due the extended approximate BO equation for this case (in fact the Baer-Englman equation) which is obtained from Eq. (12) by setting $\omega_j=1$.

Let us summarize what was done so far: We derived the three adiabatic coupled BO equations [see Eq. (9)] for a tristate two-coordinate model that we intend to study, as well as the corresponding extended approximate BO equations [see Eq. (12)]. In addition, we presented a set of two equations [see Eq. (9b)] which follows from Eqs. (9) by dropping the interaction of the two-state system with the third state (i.e., assuming $\eta=0$). The extended approximate BO equation for this case is also given in Eq. (12) by assuming $\omega_j=1$ (instead of 2 or zero).

B. Diabatic framework

One of the main obstacles in solving Eqs. (9) and (9b) is the existence of nonadiabatic singular terms which make the numerical procedure very unstable. Therefore, it was suggested, some time ago [9,11], to eliminate these terms by an orthogonal transformation—the ADT matrix—which forms the diabatic framework. This ADT matrix A fulfils the following first-order differential equation [9,11]:

$$\boldsymbol{\nabla}A+\boldsymbol{\tau}A=\mathbf{0}. \tag{13}$$

The conditions for this equation to have a solution are discussed in the Appendix in (I). The A matrix is solely determined by the τ matrix (and boundary conditions), but its physical relevance is decided upon its ability to form continuous, uniquely defined diabatic potentials $W(q,\varphi)$ which follows from the ADT:

$$W(q,\varphi)=A^*(q,\varphi|q_0,\varphi_0)u(q,\varphi)A(q,\varphi|q_0,\varphi_0). \tag{14}$$

In this equation $u(q,\varphi)$ is the adiabatic potential matrix assumed to be continuous and uniquely defined throughout configuration space. Section II was devoted to this problem, and we made sure that the τ matrix, constructed in the Sec. III A, will indeed yield diabatic potentials as required.

The ADT matrix of a two-state case [to transform Eq. (9b)] was discussed on many occasions [9,11], so that here we just mention it for the sake of completeness:

$$A=\begin{pmatrix}\cos\theta & \sin\theta\\ -\sin\theta & \cos\theta\end{pmatrix}, \tag{15}$$

where θ for our model is [see also Eqs. (7) and (8)]

$$\theta=\int_0^{\varphi}t(\varphi')q\,d\varphi'=\frac{\varphi}{2}. \tag{16}$$

To derive the tristate ADT matrix, the A matrix is presented as a product of three matrices of the type given in Eq. (15) [6,12],

$$A(\theta_{12},\theta_{23},\theta_{13})=A^{(12)}(\theta_{12})A^{(23)}(\theta_{23})A^{(13)}(\theta_{13}), \tag{17}$$

where the matrix $A^{(12)}(\theta_{12})$ is defined as

$$A^{(12)}(\theta_{12})=\begin{pmatrix}\cos\theta_{12} & \sin\theta_{12} & 0\\ -\sin\theta_{12} & \cos\theta_{12} & 0\\ 0 & 0 & 1\end{pmatrix}, \tag{18}$$

and the other two matrices are defined in a similar way except that the position of the 1 is shifted along the diagonal. As shown by Top and Baer, [12], following Eq. (13), the three angles fulfill the three coupled first-order equations

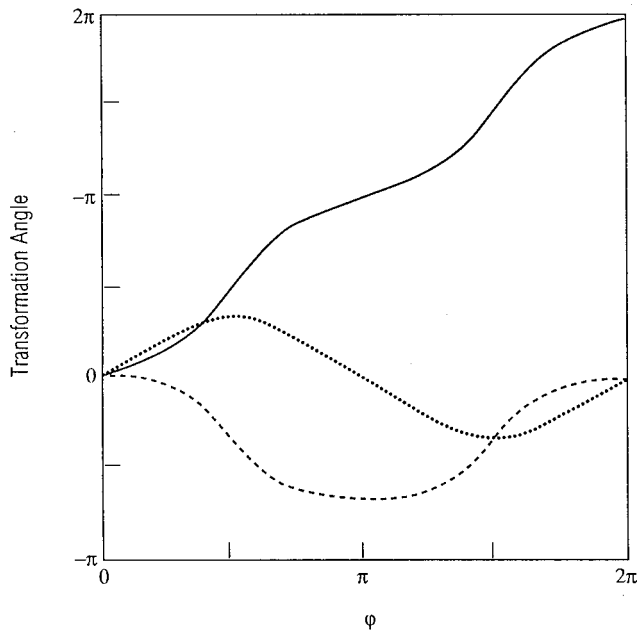

FIG. 1. The three adiabatic-to-diabatic transformation angles as obtained by solving Eqs. (20): ------, θ_{12}; ——, θ_{23}; ·····, θ_{13}.

$$\nabla\theta_{12} = -t_1 - \tan\theta_{23}(-t_2\cos\theta_{12} + t_3\sin\theta_{12}),$$

$$\nabla\theta_{23} = -(t_3\cos\theta_{12} + t_2\sin\theta_{12}), \tag{19}$$

$$\nabla\theta_{13} = -(\cos\theta_{23})^{-1}(-t_2\cos\theta_{12} + t_3\sin\theta_{12}),$$

where the t_j, $j=1,2,3$, were introduced in Eq. (2). For the present choice of the t_j's [see Eqs. (7) and (8)], we obtain the following equations:

$$\nabla\theta_{12} = -\frac{1}{q}t_0(1+\eta\sin\theta_{12}\tan\theta_{23}),$$

$$\nabla\theta_{23} = -\frac{1}{q}\eta t_0\cos\theta_{12}, \tag{20}$$

$$\nabla\theta_{13} = -\frac{1}{q}\eta t_0\sin\theta_{12}(\cos\theta_{23})^{-1}.$$

It is noted that the third equation is decoupled from the other two (this, by no means, implies that the angle θ_{13} is less important than the two other angles). In fact, to guarantee the correct topological features, all three matrices in Eq. (17) have to be derived and to be included in the product.

Equations (20) were solved for the present case where $t_0=\frac{1}{2}$ and $\eta=\sqrt{3}$, and for

$$\nabla = \frac{1}{q}\frac{\partial}{\partial\varphi}. \tag{21}$$

The φ-dependent θ_{ij} angles, in the range $[0, 2\pi]$, are shown in Fig. 1. It is noted that the two angles end up, following a complete cycle, with the value zero, and one of them with the value 2π. Thus the A matrix does not change sign [see Eq. (17)] while completing a cycle. This is in contrast to the two-state case with $t_0=\frac{1}{2}$, where the corresponding angle becomes π and the A-matrix changes sign [see Eqs. (15) and (16)].

TABLE I. Adiabatic potential-energy parameters used in the calculations.

m	0.58 amu
A	3.0 eV
D_2, D_3	0.5 eV, 10.0 eV
σ	0.30 Å
σ_0	0.75 Å
ω_0	$39.14\times10^{13}\,s^{-1}$
$\overline{\omega_0}$	$7.83\times10^{13}\,s^{-1}$

Once the A matrix is known, employing Eq. (14) we can obtain the diabatic potential W matrix and solve the relevant diabatic Schrödinger equation (SE), which is of the form [9,11].

$$T\Xi + (W - IE)\Xi = 0, \tag{22}$$

where $\Xi = A^*\Psi$, and I is the unit matrix.

C. Adiabatic potential-energy matrix

For the present model we assumed a two-arrangement channel potential similar to the one employed in the previous two-state studies [3–5]. Moreover, the two lowest states are identical to the ones employed before, namely,

$$u_1(R,r) = \tfrac{1}{2}m[\omega_0 - \omega(R)]^2r^2 + Af(R,r) \tag{23a}$$

and

$$u_2(R,r) = \tfrac{1}{2}m\omega_0^2r^2 - (D_2 - A)f(R,r), \tag{23b}$$

where m ω_0, A, and D_2 are constants (their values are listed in Table I), R and r are Cartesian coordinates (defined in the intervals $-\infty\leqslant R\leqslant\infty$ and $-\infty\leqslant r\leqslant\infty$) related to q and φ in the following ways:

$$R = q\sin\varphi \quad \text{and} \quad r = q\cos\varphi. \tag{24}$$

The function $f(R,r)$ is chosen to be a two-variable Gaussian which peaks at (0, 0), namely,

$$f(R,r) = \exp\left(-\frac{R^2+r^2}{\sigma^2}\right), \tag{25}$$

and $\omega(R)$ is a an R-dependent frequency given in the form

$$\omega(R) = \overline{\omega_0}\exp\left(-\frac{R^2}{{\sigma_0}^2}\right). \tag{26}$$

The values of σ and σ_0 are also listed in Table I. The third surface u_3 is chosen to be similar to u_2 defined for a different D value, namely, for $D_3=10$ eV. In Fig. 2 we present the two-dimensional three adiabatic potential-energy surfaces. It can be seen that this potential describes a two-arrangement channel system; the reagent-arrangement defined for $R\to\infty$ and a product-arrangement defined for $R\to-\infty$.

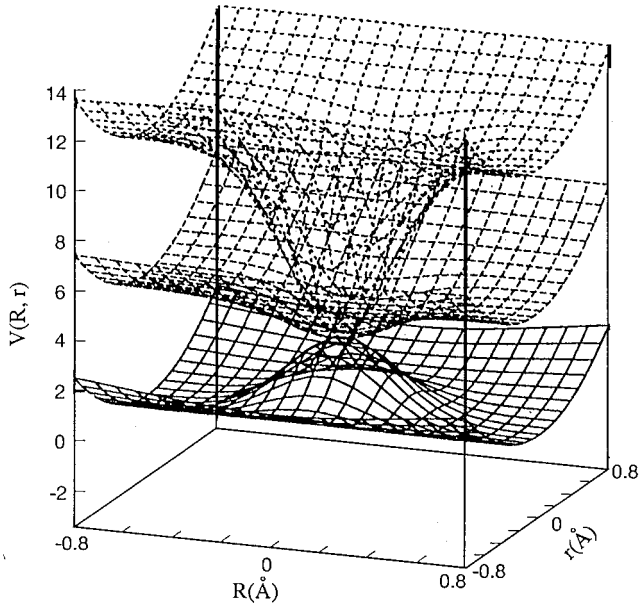

FIG. 2. The three adiabatic potential-energy surfaces that were applied in the present study.

This completes the derivation of the model. In Sec. IV we present the results due to the various sets of equations, particularly Eq. (9) [or its diabatic counterpart given in Eq. (22)], Eq. (9b) (or its diabatic counterpart presented in Refs. [3], [5]), and Eq. (12) for three different cases, namely, ω_j; $j=1,2,3$.

IV. RESULTS AND DISCUSSION

In order to obtain the transition probabilities, the various SEs mentioned in Sec. III were solved using the wave-packet time-dependence approach. This approach was fully described in Ref. [5], and will not be repeated here. The results are presented in two tables: the inelastic probabilities are given in Table II, and the reactive ones in Table III.

The calculations were done for four energies, i.e., $E=1.0$, 1.5, 2.0, and 2.5 eV, all of them below the upper surfaces and thus below the common intersection point of the three surfaces which takes place at $E=3.0$ eV. We shall report on transitions from the ground vibrational state only. Five different types of probabilities will be shown for each transition: (a) Probabilities due to a full tristate calculation, carried out within the diabetic representation, employing Eq. (22). (b) Probabilities due to a two-state calculation (for

TABLE II. Nonreactive state-to-state transition probabilities.

$0\rightarrow0$	$0\rightarrow1$	$0\rightarrow2$	$0\rightarrow3$	$0\rightarrow4$	$0\rightarrow5$	$0\rightarrow6$	$0\rightarrow7$	$0\rightarrow8$
				$E=1.00$ eV				
0.3511[a]	-	0.6434	-					
0.3515[b]	-	0.6411	-					
0.3404[c]	-	0.6574	-					
0.3473[d]	-	0.6509	-					
0.2762[e]	-	0.6916	-					
				$E=1.5$ eV				
0.1913	-	0.3231	-	0.3419				
0.1918	-	0.3184	-	0.3389				
0.2065	-	0.3195	-	0.3304				
0.1962	-	0.3202	-	0.3397				
0.3172	-	0.2422	-	0.2773				
				$E=2.0$ eV				
0.2304	-	0.1515	-	0.1713	-	0.0894		
0.2357	-	0.1470	-	0.1664	-	0.0900		
0.2305	-	0.1587	-	0.1808	-	0.0784		
0.2409	-	0.1463	-	0.1691	-	0.0918		
0.2745	-	0.1481	-	0.0962	-	0.0406		
				$E=2.5$ eV				
0.0955	-	0.1188	-	0.0900	-	0.0512	-	0.0359
0.1198	-	0.1199	-	0.0652	-	0.0350	-	0.0126
0.1051	-	0.1199	-	0.0813	-	0.0434	-	0.0328
0.1173	-	0.1088	-	0.0613	-	0.0323	-	0.0126
0.1559	-	0.1161	-	0.0642	-	0.0377	-	0.0323

[a]Trisurface calculation.
[b]Two-surface calculation.
[c]Single-surface calculation ($\omega=2$).
[d]Single-surface calculation ($\omega=1$).
[e]Single-surface calculation ($\omega=0$); the ordinary BO approximation.

TABLE III. Reactive state-to-state transition probabilities.

$0\rightarrow0$	$0\rightarrow1$	$0\rightarrow2$	$0\rightarrow3$	$0\rightarrow4$	$0\rightarrow5$	$0\rightarrow6$	$0\rightarrow7$	$0\rightarrow8$	$0\rightarrow9$
				$E=1.00$ eV					
0.0044[a]	-	0.0063	-						
-	0.0049[b]	-	0.0079						
0.0047[c]	-	0.0195	-						
-	0.0045[d]	-	0.0080						
0.0094[e]	-	0.0362	-						
				$E=1.5$ eV					
0.0325	-	0.0592	-	0.0311					
-	0.1068	-	0.0256	-	0.0068				
0.0419	-	0.0648	-	0.0308	-				
-	0.1078	-	0.0248	-	0.0075				
0.0644	-	0.0612	-	0.0328	-				
				$E=2.0$ eV					
0.1110	-	0.0279	-	0.0319	-	0.2177			
-	0.1232	-	0.03333	-	0.0633	-	0.1675		
0.1068	-	0.0172	-	0.0274	-	0.2277	-		
-	0.1264	-	0.0353	-	0.0656	-	0.1678		
0.1351	-	0.0217	-	0.0304	-	0.2647	-		
				$E=2.5$ eV					
0.1318	-	0.0295	-	0.0091	-	0.1375	-	0.2043	-
-	0.0936	-	0.0698	-	0.1350	-	0.0200	-	0.2398
0.1256	-	0.0155	-	0.0084	-	0.1545	-	0.1977	-
-	0.0947	-	0.0658	-	0.1363	-	0.0190	-	0.2367
0.1831	-	0.0343	-	0.0089	-	0.1607	-	0.1157	-

[a]Trisurface calculation.

[b]Two-surface calculation.

[c]Single-surface calculation ($\omega=2$).

[d]Single-surface calculation ($\omega=1$).

[e]Single-surface calculation ($\omega=0$); the ordinary BO approximation.

which $\eta=0$), carried out within the corresponding diabetic representation, employing a set of equations [similar to Eq. (22)] discussed elsewhere [3,5], (c) Probabilities due to a single state equation presented in Eq. (12) for $\omega_j=2$. (d) Probabilities due to a single state equation presented in Eq. (12) for $\omega_j=1$. (e) Probabilities due to a single state equation presented in Eq. (12) for $\omega_j=0$ [this case is, in fact, the ordinary BO equation—see Eq. (9a)]. Out of the five cases, two (the second and the fourth) present the ordinary conical intersection (CI) case; *a priori*, we expect the two CI cases to show symmetry effects (as demonstrated in Refs. [3, 5]), and if the extended BO approximation is correctly worked out, then the other three calculations are not expected to yield any symmetry-affected results.

At this stage we would like to mention that the model, without the inclusion of the vector potential, is constructed in such a way that it obeys certain selection rules, namely, only even→even and odd→odd transitions are allowed. Thus any deviation, in the results, from these selection rules will be interpreted as a symmetry change.

The inelastic (nonreactive) processes, presented in Table II, are in general not affected by the nonadiabatic coupling terms, immaterial of what kind is used or which approximate BO equation is solved. Still we note that the ordinary BO equation yields, on certain occasions, results which are somewhat different than those due to the other equations (including its gauge invariant equation). We do not have a sensible explanation for this finding other than speculating that the time-dependent grid method as applied here becomes more cumbersome when the (singular) nonadiabatic coupling terms are included in the SE equation.

Effects due to nonadiabatic coupling terms are seen in Table III, where the two-state results and the corresponding extended approximated-BO equation results (those for $\omega=1$) transformed the even→even and odd→odd selection rules to odd↔even selection rules. This transformation was discussed at length in previous publications [3,5], and therefore will not be repeated here. The more interesting results are those for the tristate case which is also dominated by $t_0=\frac{1}{2}$, just like the two-state case, but does not produce *any* geometrical effects. This behavior was expected from the relevant extended approximated BO equation, which, as we showed, is identical to the ordinary BO equation. Nevertheless, we thought that, since the extended BO equation is still approximate, the geometrical effects could be partly wrong (they were not). Thus the present calculations revealed two facts: (a) Geometrical features do not necessarily show up where they are expected, as seen in the present tristate case. (b) The extended approximate BO equation contains the correct information regarding the geometrical effects, in the

two-state case it contains geometrical effects due to the conical intersection, and in the tristate case it tells us that such effects do not exist.

V. CONCLUSIONS

In this work we tested the extended-approximate BO equation as derived in paper I for a tristate system. For this sake a two-arrangement—two-coordinate reactive model was devised. The model consisted of three adiabatic potential-energy surfaces and a 3×3 nonadiabatic coupling matrix (of a specific form to be able to produce physical diabatic potentials). The model was solved twice: once without doing any approximation and once approximating the three coupled Schrödinger equations by the above-mentioned single (extended) BO equation. The calculations were done for energies below the lowest *excited* adiabatic potential (thus for cases where the two upper excited states are energetically forbidden). Very similar state-to-state (reactive and nonreactive) transition probabilities were obtained, indicating that the new approximate BO equation yields relevant results for a tristate system. It is important to emphasize that to our knowledge, this is the first time that such a BO approximation is applied to a system of three adiabatic Schrödinger equations coupled by singular nonadiabatic coupling terms, and is found to yield the relevant state-to-state transition probabilities.

We also found other interesting features, and one of them will be discussed next. The model was devised in such a way that in case the nonadiabatic coupling terms are ignored the allowed transitions in both channels—the reactive one and the inelastic one—are even→even and odd→odd, whereas even→odd transitions are forbidden. In a previous publications [3,5] it was shown that including nonadiabatic coupling terms related to a conical intersection changes the character of the transitions for the *reactive* channel: namely, the above-mentioned even→even and odd→odd transitions became forbidden, but then, instead, the even↔odd became allowed. Now, extending the two-state model to a tristate model, where the third state is coupled to the second state by a singular nonadiabatic coupling term, again affects the selection rules for the reactive transitions. It was found that the original selection rules which were significantly destroyed by the conical intersection are restored due to the incorporated coupling to the *third* state.

In performing this numerical study we were interested in making two points.

(1) We wanted to demonstrate the validity of the newly derived BO approximation for an N-state system which exhibits topological effects. We treated two different cases: the $N=2$ case and the $N=3$ case. In both cases the nonadiabatic coupling terms are expected to yield different topological effects. The solution of the relevant two coupled equations and the three coupled equations justified these expectations. The relevant single approximate BO equation for each of the two cases correctly reproduced the results obtained from solving the full system of Schrödinger equations.

(2) The most important outcome of this study is that one has to be very careful in correctly defining the sub-Hilbert space. Assuming that solving the relevant Schrödinger equation for two coupled states is a good approximation of a system of three coupled states may lead to erroneous results. The danger is small if the two-state system exhibits the same symmetry as does the three-state system, but irrelevant results are expected when the two and three-state systems exhibit different symmetries (the numerical example worked out in this publication is of such a feature).

Another outcome, not related to the numerical study, is the fact that we found that the topological matrix D which is a diagonal matrix and should have in its diagonal a mixture of $(+1)$'s and (-1)'s is found to be very restricted in case of $N=3$. In a recent publication [14], one of the present authors suggested a classification of topological effects according to the size N of the sub-Hilbert space. Thus for $N=2$ we encountered only two possibilities: the D matrix contains either two $(+1)$'s in its diagonal or two (-1)'s. When $N=3$, it was found that the D matrix contains either three $(+1)$'s or two (-1)'s and one $(+1)$ in its diagonal. However, the analytic treatment of our simplified model, as performed in Sec. II, yielded only the case of three $(+1)$'s in the diagonal [see Eq. (6)]. This would imply that in case of $N=3$ no topological effects are expected. However, recently, two of the present authors [6] studied a more general case for $N=3$, and found there that the topological matrix has two (-1)'s and one $(+1)$ in its diagonal, which seems to indicate that topological effects are also expected in tristate systems.

ACKNOWLEDGMENTS

One of the authors (M.B.) would like to thank Professor Y. T. Lee and Professor S. H. Lin for their warm hospitality at the IAMS, and the Academia Sinica for supporting this research.

[1] M. Baer, S. H. Lin, A. Alijah, S. Adhikari, and G. D. Billing, previous paper, Phys. Rev. A **62**, 032506 (2000).
[2] M. Baer and R. Englman, Chem. Phys. Lett. **265**, 105 (1996).
[3] R. Baer, D. Charutz, R. Kosloff, and M. Baer, J. Chem. Phys. **105**, 9141 (1996).
[4] D. Charutz, R. Baer, and M. Baer, Chem. Phys. Lett. **265**, 629 (1997).
[5] S. Adhikari and G. D. Billing, J. Chem. Phys. **111**, 40 (1999).
[6] A. Aljah and M. Baer, J. Phys. Chem. **104**, 3181 (2000).
[7] M. Baer and R. Englman, Mol. Phys. **75**, 293 (1992).
[8] M. Baer, J. Chem. Phys. **107**, 2594 (1997).
[9] M. Baer, Chem. Phys. Lett. **35**, 112 (1975).
[10] M. Baer, Mol. Phys. **40**, 1011 (1980).
[11] M. Baer, in *Theory of Chemical Reaction Dynamics*, edited by M. Baer (CRC Press, Boca Raton, FL, 1985), Vol. II., Chap. 4.
[12] Z. H. Top and M. Baer, J. Chem. Phys. **66**, 1363 (1977).
[13] M. Baer, J. Chem. Phys. **104**, 3181 (2000).
[14] M. Baer, Chem. Phys. Lett. **322**, 520 (2000).